ARTICLE NO. 79-4123

Investigation of Acoustic Radiation from Supersonic Jets by Double-Pulse Holographic Interferometry

Ahmet Ozkul*
The George Washington University, Hampton, Va.

A new experimental method was used to investigate optically the acoustic field radiated from supersonic jets. The method utilizes a pulse ruby laser to obtain double-exposure holograms of the sound field of a supersonic jet. The jet remains on during both exposures, thus eliminating the no-flow exposure. The time separation between the pulses can be varied to observe different spectral components of the radiation. Optical records were obtained for free supersonic jets issuing from contoured nozzles with exit Mach number 1.0, 1.5, and 2.0. The supersonic jets were operated under both off-design and fully expanded shock free conditions. It was found that high-frequency acoustic radiation originates mainly from the regions near the nozzle exit, whereas the low-frequency noise is generated from regions further downstream. These findings are consistent with the acoustic data obtained by other investigators. An analysis using a two-dimensional sound field was made to illustrate the underlying principle of the present experimental technique for interpreting the optical data gathered from the sound field of jet flows as well as all other potential applications.

I. Introduction

THE work of Lighthill[1,2] has provided a firm theoretical basis for the study of sound induced by aerodynamic effects. Specifically, Lighthill theorized that the sound radiation from a turbulent air jet can be described by a prescribed stress distribution in the fluid flow in terms of acoustic quadruple sources. Suitable approximations of this quadruple distribution can then yield a reasonably accurate estimate of overall characteristics of the sound field.

Alternate approaches have also been developed by various investigators to formulate the acoustic characteristics of supersonic jets. Among these Phillips was the first one to consider the noise radiation from supersonic turbulent shear flows.[3] He theorized the mixing region as being composed of random distribution of eddies which are convected downstream with a range of velocities. Whenever the velocities of these eddies attain values which are supersonic relative to the surrounding environment they carry with them weak shock fronts. These fronts were shown to be highly directional, oriented in such a way that their apparent angle of propagation with the jet axis was very close to that of a Mach angle:

$$\theta = \cos^{-1}(1/M_c), \quad M_c = V_e/a_0$$

where V_e is eddy convection velocity. Ffowcs Williams[4] also viewed the supersonic mixing layer as the major noise producing mechanism in supersonic jets.

Ribner[4] considered the radiated sound from supersonic jets using a two-dimensional square eddy distribution within the shear region of the jet. Sedelnikow,[5] Tam,[6] and Liu[7] also considered the disturbances as instability waves propagating the shear layer.

More recent studies by various investigators[7,8] theorize that there are two scales of instability waves in a supersonic jet. The first one is in the form of Mach waves which occur at high frequencies. These waves have a scale of the shear layer thickness. Second, there exist much larger-scale undulations encompassing the entire jet. Previously obtained optical records using conventional techniques seem to indicate that the aforementioned large-scale instability takes on a spiral motion along the axis, and it appears to be similar to those instability waves observed in laminar or transition flow. These investigators also believe that these large-scale instabilities are the major contributing noise mechanism in supersonic jets.

In 1965, Lowson's[8] optical studies provided additional information on supersonic jet noise radiation and generation mechanisms. Lowson as well as some other subsequent investigators provided shadowgraphic evidence which demonstrated the presence of nozzle centered and shock-turbulence related strong wavefronts of a spherical nature. The most prominent wave form in their test results was found to be the nozzle centered lip radiation associated with the transition of the boundary layer very near the nozzle exit and also (for jets operating at off-design conditions) spherical waves appeared to be centered on shock-mixing layer intersections and propagating transverse to the jet axis. In addition to Lowson's experimental investigation by shadowgraph technique, optical data in the form of spark Schlieren pictures have also been reported on the sound field generated by freejets. The results obtained[9,10] demonstrated the presence of the Mach waves discussed earlier.

A better technique for acoustic field visualization from free supersonic jets was first obtained by Salant[11] using double-exposure holographic interferometry. In Salant's method, the doubly exposed interferograms were obtained by exposing the film plate twice holographically. The first exposure was made without the jet flow in the test area. This exposure records the no-flow ambient conditions and serves as the reference state. After this first exposure, the jet is turned on to a specified operating condition, and a second exposure is made. By analyzing the obtained holograms, Salant concluded that the oblique fronts visible in the near acoustic field are Mach waves and that they are the most dominant radiation present in the acoustic field of a free supersonic jet. Furthermore, his results indicated that Mach waves do not originate within the mixing region, but rather at or within the jet core itself. Also,

Received Oct. 27, 1978; revision received April 9, 1979.

Index categories: Aeroacoustics; Noise.

*Joint Institute for Advancement of Flight Sciences. Presently, Technical Staff Member, International Telecommunication Satellite Organization, Washington, D.C.

the straightness and lateral content of the Mach waves, as well as relatively high measured convective velocities (0.8-0.9 V_{jet}) within the mixing region, convinced him that although Mach wave radiation does in fact dominate the acoustic field of supersonic jets, it may be incorrect to model the generating mechanism as a convected turbulence (i.e., eddy) effect. Rather, it may be more appropriately described in terms of jet instabilities.

In the present technique, in contrast to Salant's method, the jet flow remains on during both of these exposures and there is a controlled time separation between the two exposures. Holograms obtained from the present method reveal more information within both flow and acoustic fields of a supersonic jet than do those obtained using Salant's method. Specifically, the present study provides an image of the jet acoustic field and flowfield by relating the time interval between two exposures to the spatial density pattern observed in the reconstructed image. Furthermore, because of the short pulse separations employed, the present technique suppresses experimental errors that may result from such anomalies as the relative movement of optical components and change of ambient conditions between exposures. Such factors may introduce significant errors in the method employed previously by Salant.

Despite the fact that an instability model as pointed out earlier prevails in the current literature as being the major noise mechanism in supersonic flows, questions such as the scale of instabilities, their spectral characteristics, the existence of other forms of noise mechanisms and the interrelationship among various mechanisms remain unanswered. The goal of the present investigation is to shed light on these questions as well as to study the prospective applications of the double-pulse holographic interferometry in experimental mechanics.[12] By using a holographic technique as described in the next chapter, the noise field and flowfield of a cold supersonic laboratory scale jet operated under fully over- and underexpanded modes are studied. For a better understanding of the observed optical data, a simple analysis is made on the experimental method used.

II. Brief Theory of Double-Exposure Holography

The single-exposure holograhic interfermetry, which uses a laser as a coherent light source, responds directly to the density field present during the time of exposure. Double-exposure transmission holography, however, involves the linear superposition of two or more hologram exposures. Since each hologram forms an interference pattern completely independently of the others, linear image superposition can be obtained either by repetitively exposing the same film plate during recording or by aligning two or more singly exposed holograms to form a desired interference pattern during image reconstruction. In the holographic interferometry method used in the present study, the flowfield and acoustical field are exposed twice holographically with a preselected time separation between the two exposures (Fig. 1). The jet remains on during both exposures, allowing the hologram plate to record two consecutive instantaneous density fields separated by the preselected time interval. The pulse separation employed may be varied.

The physical mechanism that yields the interferogram is the relative phase change of the scene beam as it travels through the test area during each exposure. The phase change is related to the difference in the density field within the test area between the two exposures. Thus, the present double-pulse holographic interferometry responds directly to the density differential between the two exposures.

It can be shown that[12] the relative phase change of the scene beam wavefront between the two exposures $\Delta\phi(r)$ which yields the interferometric pattern can be given by

$$\Delta\phi(r) = 2\pi q(x,y,z) \tag{1}$$

where q is the path length change of the scene beam between two exposures. In terms of multiples of the laser wavelength q is given by

$$q(x,y,z) = \frac{1}{\lambda_0}\int_0^L \{n_2(x,y,z) - n_1(x,y,z)\}\,dz \tag{2}$$

where

z = direction of scene beam propagation (Fig. 1)
λ_0 = laser wavelength (ruby laser; $\lambda_0 = 6943$ Å)
L = extent of density region
n_2 = three-dimensional index of refraction field during second exposure
n_1 = three-dimensional index of refraction field during first exposure

The index of refraction of a gas is a function of the gas density given by:

$$n \simeq 1 + \beta(\rho/\rho_0) \tag{3}$$

For air under standard conditions, $\rho_0 = 0.0012929$ gm/cm^3 and $\beta = 0.000291$ (Gladstone Dale constant).

Substituting Eq. (3) into Eq. (2)

$$q(x,y,z) = \frac{1}{\lambda_0}\frac{\beta}{\rho_0}\int_0^L \{\rho_2(x,y,z) - \rho_1(x,y,z)\}\,dz \tag{4}$$

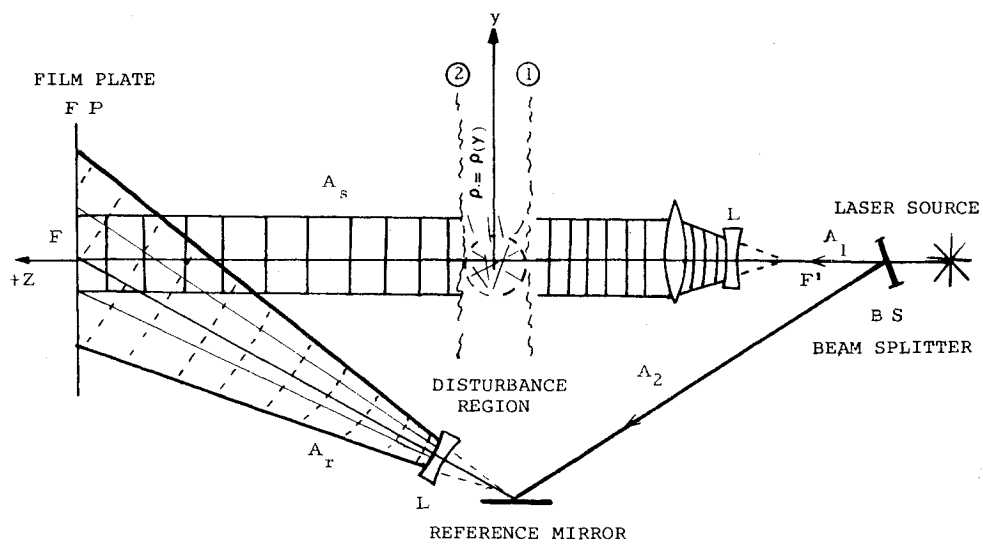

Fig. 1 A typical transmission holography optical arrangement used in the investigation of acoustic radiation from supersonic turbulent jets.

where ρ_2 and ρ_1 are the instantaneous density fields at the first and second exposures, respectively.

For fringe formation,

$$\Delta\phi(r) = (2m'+1)\pi, \quad m'=0, \pm 1, \pm 2, \pm 3... \tag{5}$$

must be satisfied. From Eq. (1)

$$(2m'+1)\pi = 2\pi q(x,y,z) \tag{6}$$

or

$$(2m'+1)\pi = 2\pi \frac{\beta}{\lambda_0 \rho_0} \int_0^L \{\rho_2(x,y,z) - \rho_1(x,y,z)\}\,dz \tag{7}$$

In order to derive an expression relating the sensitivity of the present technique to various test parameters, a two-dimensinal density field will next be considered (i.e., spatial density variation along the z direction is negligible).

Then, from Eq. (4)

$$q(x,y) = \frac{1}{\lambda_0}\frac{\beta}{\rho_0}\{\rho_2(x,y) - \rho_1(x,y)\}L \tag{8}$$

This means

$$\Delta\rho(x,y) = \{\rho_2(x,y) - \rho_1(x,y)\} = (2m'+1)\frac{\rho_0}{L\beta}\frac{\lambda_0}{2} \tag{9}$$

Equation (9) says that a fringe will be formed whenever the density change $\Delta\rho$ between the two exposures is equal to or greater than

$$\Delta\rho_t = \frac{\rho_0}{L\beta}\frac{\lambda_0}{2} \tag{10}$$

Hence, $\Delta\rho_t$, can be defined as the "threshold density difference." ($\Delta\rho_t$ corresponds to 140-dB pressure level differential, re: 0.0002 microbar, for $L = 30$ cm.).

Since interferometric methods cannot detect the sign of the density difference, the integer m' may be restricted to only positive integers (including 0), i.e.,

$$|\Delta\rho| = (2m'+1)\frac{\rho_0}{L\beta}\frac{\lambda_0}{2}, \quad m'=0,1,2,3... \tag{11}$$

From Eq. (11) it may be deduced that a dark fringe forms at those (x,y) positions where the absolute value of the density difference between the two exposures is an odd integer multiple of the threshold density difference.

In order to relate the analysis developed here to the detection of acoustic waves using double-pulse holographic interferometry, it will next be assumed that the density field to be observed is a harmonic plane acoustic wave traveling normal to the direction of the laser light. Then,

$$\rho(y) = \rho_0 + \rho e^{i\{ky - \omega t + \phi\}}$$

where

$\rho(y)$ = density variations due to acoustic wave motion
ρ = wave amplitude
$k = \omega/a_0$ (a_0 = speed of sound)
ϕ = arbitrary reference phase

It can be shown[12] that the first-order dark fringes (i.e., $m'=0$) will be observed in the reconstructed image at those y positions where

$$|\Delta\rho(y)| = \frac{\rho_0}{\beta L}\frac{\lambda_0}{2} \tag{12}$$

However, since

$$\Delta\rho(y) = \rho_2(y) - \rho_1(y) = \rho e^{i(ky+\phi)}\{e^{-ika_0\Delta t} - 1\} \tag{13}$$

max. $|\Delta\rho(y)|$ will occur if $\Delta t = (2m'+1)T/2$, where T is the period of the acoustical wave, Δt is the time separation between pulses, and m' takes on positive values including zero. Therefore,

$$\text{max. } |\Delta\rho(y)| = 2\rho\cos(ky+\phi)$$

Physically, Eq. (13) says that in the case of an acoustic plane wave, the occurrence of the second pulse some odd multiples of the half-periods later insures that $|\Delta\rho|$ has its maximum amplitude of 2ρ sinusoidally varying in y. If 2ρ is less than the threshold density difference $|\Delta\rho_t|$ as defined by Eq. (11), no dark fringes will appear in the reconstructed image. If 2ρ is equal to $\Delta\rho_t$, however, then there will be a fringe formation separated by $\lambda/2$ along y in the reconstructed image, where λ is the wavelength of the pure tone acoustic wave. If 2ρ is greater than threshold density difference, higher-order fringes will be formed. This implies that the spacing between adjacent fringes measured in the reconstructed image should correspond to a half-wavelength of the acoustic wave as illustrated in Fig. 2. Conversely, Eq. (13) also suggests the possibility of extracting the information on fluctuating density field at a given frequency of frequency band if the appropriate time separation Δt is employed. This possibility as revealed in Eq. (13) has essentially motivated the present experimental investigation of the fluctuating density field of supersonic jets using double-pulsed holographic interferometry. For a complete interpretation of the data obtained, a more detailed analysis taking into account the

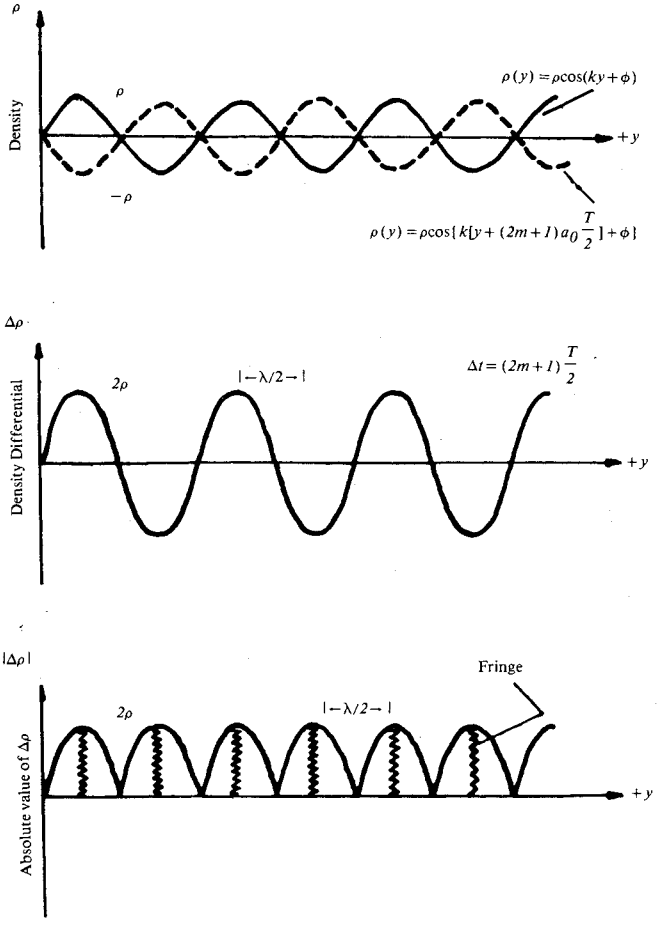

Fig. 2 Application of double-pulse holography to a propagation acoustic wave.

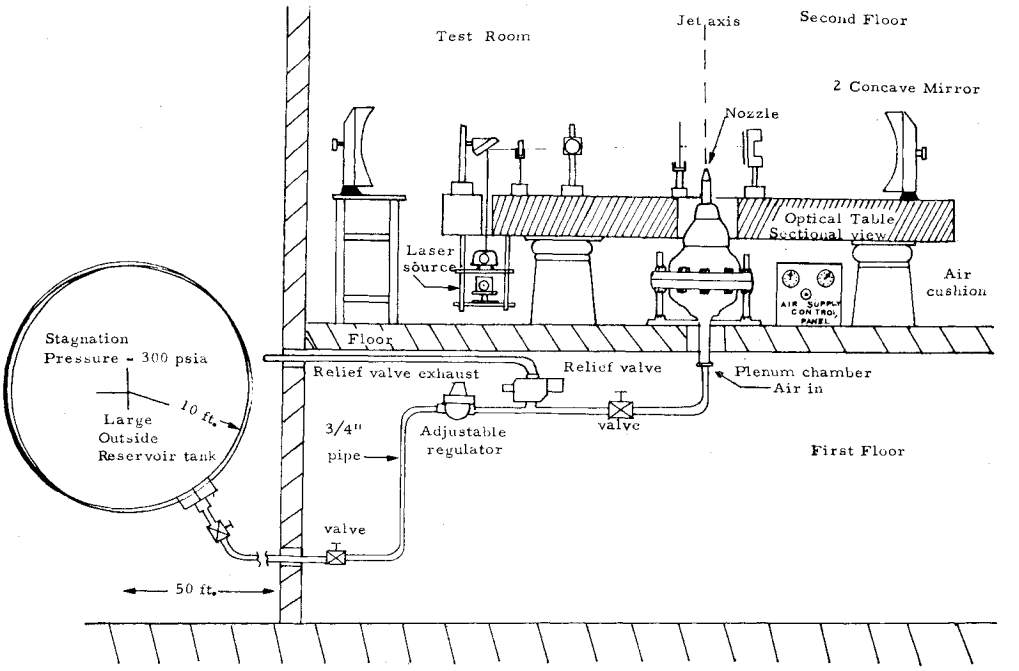

Fig. 3a Air supply system and jet apparatus.

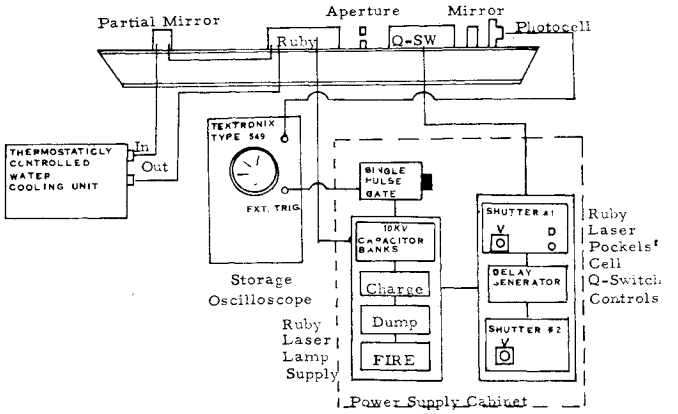

Fig. 3b Block diagram of the pulse laser hardware.

random nature of the density variation both in time and space should be carried out.[12]

It should be noted here that the present technique can be used as a powerful testing tool in experimental investigations of various aeroacoustics problems such as rotor noise, duct flow, any type of turbulent flow, and temperature varying fields offering considerable advantages over the existing methods. Specifically, the present method offers advantages over the flow visualization methods such as shadowgraph, Schlieren, and Mach Zender interferometry. The first two of these methods respond to the first and second spatial derivatives of the density field, and hence the interferograms obtained overemphasize waves of short wavelength and will weigh the steep wavefronts more heavily than smooth wavefronts. Similar to the present technique, Mach Zender interferometry responds to the density field itself. In all of the existing methods, however, the exposure times employed to "freeze" the flow are much longer, in the order of microseconds compared to nanoseconds exposure times used in the present technique, which results in spurious fringe surpression capability even under severe conditions. Furthermore, in holography a real-time interferometric observation of the density fluctuations in a given field can be obtained with a relative ease. Also, using proper optical instruments the present technique can yield "nearly" three-dimensional interferograms during a single exposure cycle, hence providing valuable information on the acoustic and flowfields of the object scene.[12] By exposing the recording media twice with a controlled time separation between exposures as used in the present investigation, double-exposure holography can automatically filter out nonfluctuating components showing only specific fluctuating components within a given density field.

It should also be mentioned here that although the present technique can be used as a powerful tool in experimental investigation of time-space varying density fields due to such mechanisms as thermal, acoustical, and mechanical sources, the conversion of the recorded fringe patterns into density profiles is a laborious and time-consuming process.

III. Experimental Apparatus and Technique

A schematic diagram of the test setup as used in the present investigation is shown in Fig. 3. Compressed air is supplied by a plenum chamber located underneath a massive optical table (Fig. 3a). The maximum stagnation pressure available is 300 psia. The table is suspended on air cushions to eliminate any unwanted vibrations. There is no confined test section for the jet flow, and the jet exhausts into the ambient air freely. The lab room has proper exhausting windows to eliminate the possible increase in the ambient pressure due to the jet exhaust.

The optical setup used is a standard transmission holography configuration and it is kept unchanged for all of the test runs. The area of the flowfield that is covered by the hologram is approximately 30 cm above the table top and the scene beam passes through a diffusive ground glass plate to provide a more uniform illumination.

The coherent light source used in these tests is a TRW model KlQDH, 10 kV, Q-switched ruby laster ($\lambda = 6943$ Å) with two Pockells cell controls. It is capable of delivering two repetitive pulses within a single firing cycle with controls on the time separation between the pulses (4 ns,-500 μs, continuous), the relative amplitude of the pulses, and the total energy output. A 1.4-mm aperture positioned in the ruby laser cavity allows only the central portion of the otherwise 1-cm-diam beam to be used. A He-Ne CW laser located in line with the pulse laser is used for alignment and the pulse laser output is recorded on a storage-type oscilloscope (see Fig. 3b) through a photocell unit housed behind the Pockells cells within the pulse laser cavity.

In order to make a holographic interferogram of the acoustic field and flowfield of a jet, the following procedure is used; the jet is turned on and stabilized to the prescribed operating conditions and the laser power supply is energized after triggering mechanisms are set to give a desired pulse separation and amplitude. After the power supply capacitors attain enough energy, the firing button is activated, thus exposing the film plate twice with each exposure of approximately 20-ns duration. The hologram plate is then removed and developed. It should be noted that in the present investigation the jet remains on during both exposures, and therefore the recorded composite interferogram is due to the superposition of the two images produced by the two different density fields occurring in the test section with Δt-s time separation.

IV. Results and Discussion

The optical records of the holograms obtained for $M=1.0$, $M=1.5$, and $M=2.0$ nozzles operating under fully, over- and underexpanded conditions are given in Figs. 4-9, inclusive. In these records the dark fringes correspond to the constant density differential contours. It should be noted here that the permanent optical recording and photographic processing of the holograms obtained from the present investigation result in the distortion of the photographs of the interferograms. This distortion effect is estimated to be approximately 15% demagnification of the original image as observed in holograms.

Figure 4 shows the fringe pattern produced by a fully expanded $M=2.0$ jet (characteristic frequency $V/D=45$ kHz). It is observed in these pictures as well as some others that, as

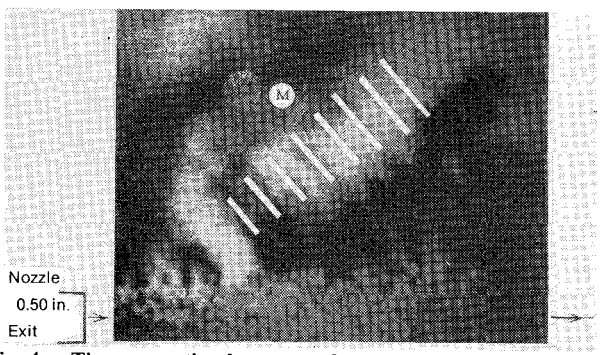

Fig. 4a Time separation between pulses ($\Delta t=25$ μs); M = frequency-dependent Mach waves.

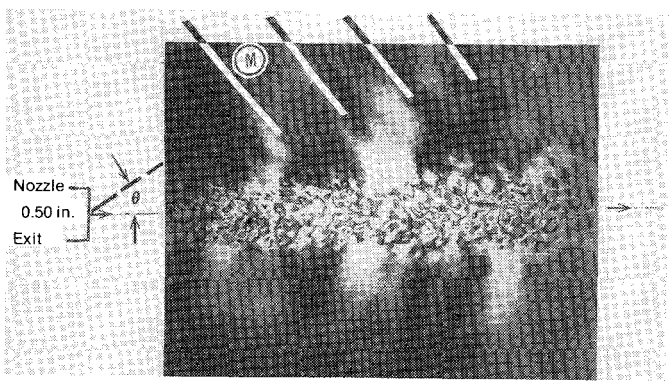

Fig. 4b Time separation between pulses ($\Delta t=50$ μs); M = frequency-dependent Mach waves; θ = Mach wave angle.

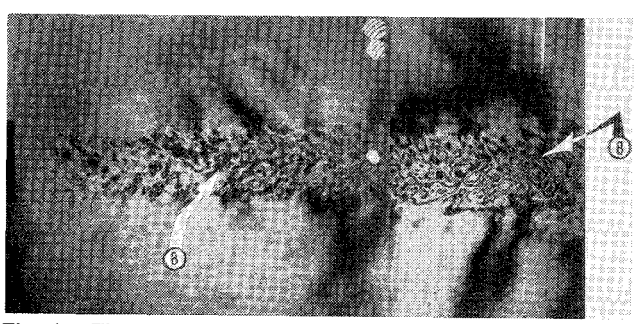

Fig. 4c Time separation between pulses ($\Delta t=100$ μs); B = closed-loop fringes related to flow disturbance.

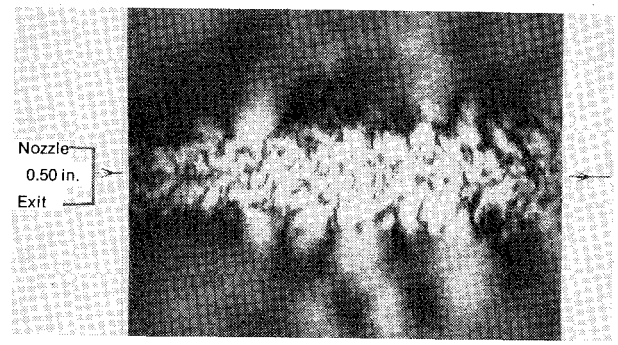

Fig. 5a Time separation between pulses ($\Delta t=25$ μs).

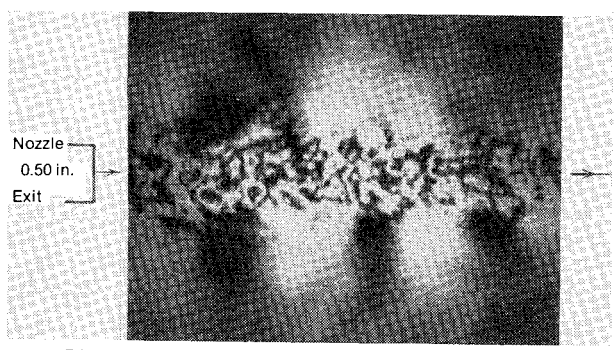

Fig. 5b Time separation between pulses ($\Delta t=50$ μs).

Fig. 5c Time separation between pulses ($\Delta t=100$ μs).

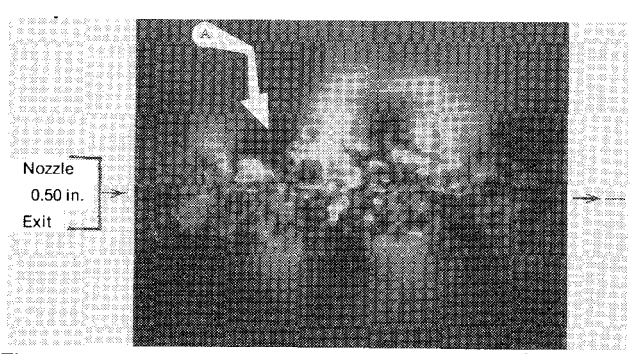

Fig. 5d Time separation between pulses ($\Delta t=500$ μs); A = large-scale (spiraling) instability waves.

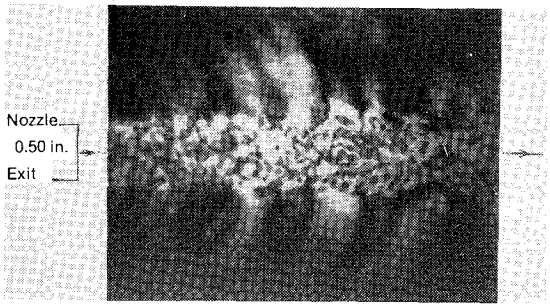

Fig. 6a Holographic interferogram of an overexpanded supersonic air jet; nozzle design Mach No. = 2.0; design $P = 100.3$ psig; oper. $P = 25.0$ psig.

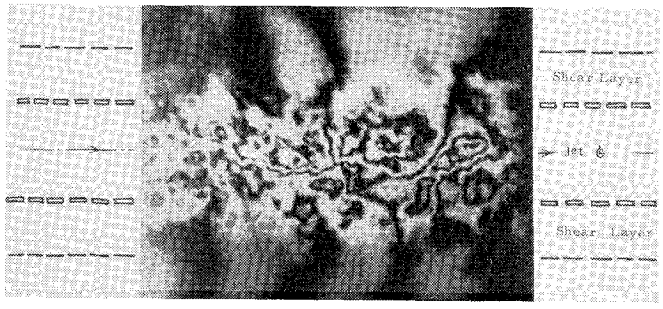

Fig. 6b Holographically enlarged interferogram of the core region; nozzle design Mach No. = 2.0; design $P = 100.3$ psig; oper. $P = 75$ psig; time separation between pulses (Δt) = 150 μs.

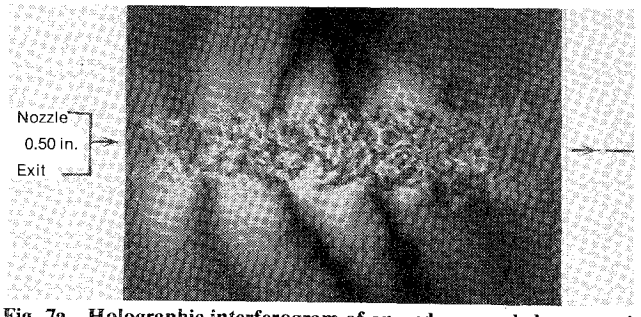

Fig. 7a Holographic interferogram of an underexpanded supersonic air jet; nozzle design Mach No. = 1.5; design $P = 39.3$ psig; oper. $P = 50$ psig.

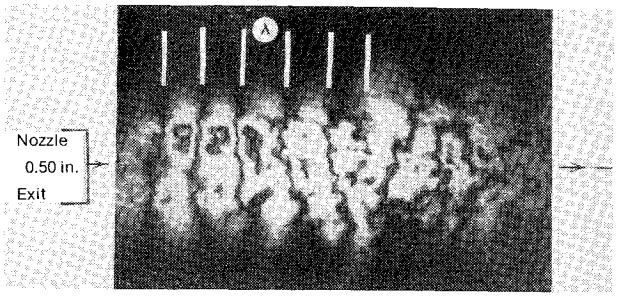

Fig. 7b Holographic interferogram of an overexpanded air jet; nozzle design Mach No. = 1.5; design $P = 39.3$ psig; oper. $P = 20.0$ psig; time separation between pulses (Δt) = 150 μs; λ = effective wavelength of the jet flow instability.

Fig. 8 Holographic interferogram of subsonic air jet, nozzle design Mach No. = 1.0; design $P = 13.0$ psig; oper. $P = 7.0$ psig; time separation between pulses (Δt) = 25 μs.

the time separation Δt is varied, a different wave structure becomes distinct in the holograms. Namely an observed spacing between the dark fringes in holograms changes as the pulse separation is varied. If these dark fringes are viewed as wavefronts, the preceding observation asserts that for each pulse separation employed, only a narrow band of sound field is enhanced by this technique. The apparent relationship between the pulse separation Δt and the observed spectral component is $\Delta t = T_n/2$, $T_n = 1/f_n$ where T_n is the period of the observed component. The typical spacing d_n between the two wavefronts (dark fringes) for a given Δt value corresponds to the half-wavelength of the spectral component observed ($d_n = \lambda_n/2$). From the foregoing observation it can be deduced that small Δt values enhance high-frequency acoustical waves in the sound field, whereas higher Δt values enhance low-frequency wavefronts. Specifically, in Fig. 4a ($\Delta t = 25$ μs, $T = 50$ μs, $f = 20$ kHz) fringe separation of approximately $\lambda/2 = 0.7$ cm, in Fig. 4b ($\Delta t = 50$ μs, $T = 100$ μs, $f = 10$ kHz) fringe separation of approximately $\lambda/2 = 1.5$ cm; and in Fig. 4c ($\Delta t = 100$ μs, $T = 200$ μs, $f = 5$ kHz) fringe separation of $\lambda/2 = 3.1$ cm are observed. It is interesting to note in Fig. 4c that the lower-frequency sound as observed in the $\Delta t = 100$ μs ($f = 5$ kHz) photograph is generated downstream of the nozzle exit, whereas the high-frequency components ($\Delta t = 25$ μs, corresponding to 20 kHz in Fig. 4a) are generated principally close to the nozzle exit. This phenomenon has been reported by many investigators in the past.

Figure 5 shows the fringe pattern produced by a fully expanded $M = 1.5$ jet (characteristic frequency $V/D = 33$ kHz). The first three pictures included in Fig. 5 shows similar information as described earlier for $\Delta t = 25$, 50, and 100-μs pulse separations. For Fig. 5d ($\Delta t = 500$ μs), however, a fringe pattern considerably different from those observed with shorter pulse separation is observed. In this figure, the undulating type of fringe structure appears to be more closely spaced than as reasoned in previous records. Although the exact nature of this discrepancy is not clearly understood it is possible as described in the previous section [i.e., $\Delta t = (2m' + 1)\Delta t$, $m' = 0,1,2,\ldots$, Eq. (13)] that when large pulse separations are utilized, the present technique, may enhance higher frequencies than expected in the optical record. The possibility of such observations for smaller pulse separation values are small, however, from both the sensitivity and resolution capabilities of the present technique. Another possible explanation for the wave structure observed in Fig. 5d is that the sound generation mechanism of low-frequency components in a free air jet may be of a spiraling motion of the flowfield around the jet axis, whose exact relationship to the sound field is not known. The possible existence of such orderly structures causing low-frequency noise generation has been suggested previously by various investigators.[7,8,12]

Figure 6a contains the hologram pictures of the $M = 2.0$ nozzle operated at the overexpanded mode. The waves emanating from the jet as seen in the hologram are believed to be shock related noise. A simple comparison indicated that the axial position of the waves as seen in the hologram agrees with those shock cell locations as observed in Schileren and shadowgraph pictures obtained using the same test configuration.

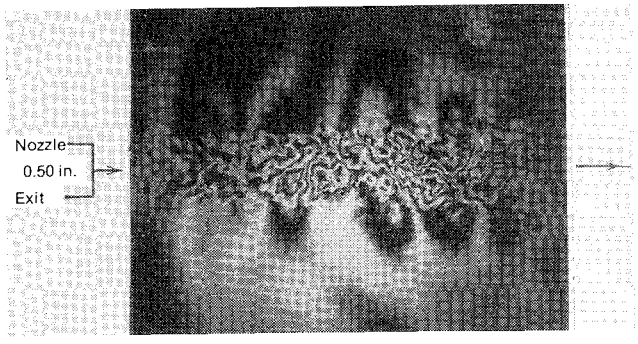

Fig. 9a Holographic interferogram of an underexpanded supersonic air jet; nozzle design Mach No. = 1.5; design $P = 39.3$ psig; oper. $P = 50$ psig; time separation between pulses (Δt) = 25 μs.

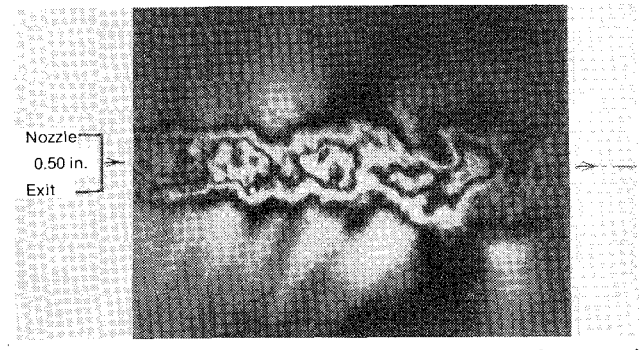

Fig. 9b Holographic interferogram of an overexpanded supersonic air jet; flow no-flow exposures; nozzle design Mach No. = 2.0; design $P = 100.3$ psig; oper. $P = 75$ psig.

The fact that the quasistationary shock structure is not visible in the holographic images indicates that the relative position of the shock structure between the two exposures does not change, or the employed pulse separation is not adequate to detect its motion. Repeated tests with different Δt values for the overexpanded $M = 2.0$ jet demonstrated that although different pulse separation results in different fringe spacing, the point of origin of fringes remained unaltered, indicating the possibility that in over- (or under-) expanded jet flows, the main noise mechanism is the shock related noise. In Figs. 4 and 6 the directional lip noise is also visible.

In an effort to visualize the initial region of the jet in more detail, an interferometric "close-up' view of an $M = 2.0$ jet flow was reproduced in Fig. 6b. This record is not an optical enlargement of one of the previous pictures in printing, but it was taken by positioning the film plate and the ground glass very close to the jet axis (approximately 5.75 cm on each side) during recording. This allows a smaller area of the flow to be recorded by the film plate, thus showing more details within the flow region. It can be noted that in this picture, as well as in some others, the oblique wavefronts seen outside the jet flow (i.e., the most dominant radiation form) can be traced into the interior of the jet, extending very close to the jet centerline. Furthermore, the longitudinal distance between the wave producing disturbances within the core seems to be evenly spaced, and these fringes appear to become wider as they traverse the shear region on each side of the jet core along the axis. Such features seem to indicate that in the case of off-design nozzle operation, these waves are the result of an instability process that takes place within the jet core, a process most likely to be related to the shock cells in the flows.

The interferometric record of the $M = 1.5$ nozzle operating at an underexpanded mode with $\Delta t = 150$ μs is given in Fig. 7a. This optical record clearly demonstrates the existence of oblique wavefronts which dominate the acoustic field of the jet on each side of the main axis. Since, in this figure, eddy-Mach wave theory based on the observed angle of inclination of these wavefronts yields an unreasonable convective eddy velocity, such modeling cannot be used in determining the origin of such waves.[3] A possible mechanism that may be responsible for this phenomenon has been suggested in the past by Powell[13] for sonic or supersonic nozzles operating under off-design conditions. Powell concluded that a powerful screech noise radiates at an upstream direction at approximately the same frequency as the disturbance passage frequency through the shock cells. When certain conditions are met, this type of noise generating mechanism becomes a self-amplifying process resulting in an instability phenomenon that produces strong wavefronts as seen in Fig. 7a.

Figure 7b contains a similar optical record for an $M = 1.5$ nozzle operated at an overexpanded mode with $\Delta t = 150$ μs. Since the employed pulse separation Δt in this test condition is the same as that for Fig. 7a, with different operating conditions, a comparison of these two optical records illustrated the variation of the noise generating mechanisms at two different modes of operation (i.e., underexpanded and overexpanded). Contrary to the underexpanded jet flow, Fig. 7b contains no wavefronts. This indicates that density fluctuations in this region are not high enough to produce a differential density value that is greater than the threshold density differential $\Delta\rho_t$, as defined earlier. The comparison of measured spectra also shows that, within a rather low-frequency range of 0-2000 Hz as well as in the high-frequency range of 4000-30,000 Hz, the overexpanded jet exhibits lower noise pressure levels than the underexpanded one. The other notable feature of Fig. 7b is visible within the flow region of the jet, where there is a rather unique and orderly fringe structure within the jet core. In this structure, the constant density differential contours appear to be equally spaced along the jet axis with secondary contours forming close to the nozzle exit. The regular pattern of the fringes within the jet core seems to diminish gradually starting about 6-diameters distance from the nozzle exit. Observation of such an orderly structure within a principally turbulent flow region of jets operating at overexpanded conditions was quite surprising. Although the basic mechanism of such a density pattern is not clearly understood, it may be interpreted as an instability phenomenon between the nozzle exit and downstream flow regions.

From the examination of Fig. 7b, it was also noticed that there exists an apparent correlation between the obtained optical data and the measured acoustic spectrum of the corresponding jet flow as follows: using standard tables, the jet velocity for the flow configuration of Fig. 7b can be found to be approximately 213 m/s. Assuming that the spacing between two adjacent fringes within the jet core corresponds to the effective wavelength of the propagating instability wave, the characteristic frequency of this process can be found as 14,000 Hz. Inspection of the measured spectra[12] however, also indicates that the intensity spectrum of this flow has a peak at a center frequency of 14,000 Hz which may correspond to that obtained from the optical data. The second peak occurs at a center frequency of about 33,000 Hz. This simple estimate indicates that in the case of overexpanded free exhaust flows, the important noise components may be due to the instability process within the jet core region. The frequency of the instability wave seems to be in good agreement with one of the most intense acoustic components that exists in the jet noise spectrum.

Although the present study was oriented toward the investigation of supersonic jet noise phenomena, the ready availability of a nozzle designed for subsonic jet flow gave motivation to including this case in the present study as well. The picture of the hologram showing the flowfield of an air jet issuing from a nozzle with design Mach No. 1 is given in Fig. 8 ($\Delta t = 25$ μs). This picture shows that there are no waves visible in the region outside the jet flow, indicating that within

that region, density fluctuations are not strong enough to be detected by the present technique. Also, within the flowfield, there are clearly visible dark fringes, located transversely along the jet axis, while the spacing between adjacent fringes increases with downstream direction. Although no correlation was found between the observed wave spacing of the optical record of Fig. 8 and the measured acoustic intensity spectrum, such a fringe pattern may represent an "orderly" phenomenon that takes place within the initial region of the jet similar to the one described earlier in Fig. 7b.

Finally, Fig. 9 gives the holographic image obtained by flow-no-flow exposures similar to those employed by a previous investigator.[11] The previous method also uses two exposures, but these exposures are taken one with and one without the presence of flow. In the present investigation the flow remains on during both exposures.

A comparison of holographic image in Fig. 9b, with that obtained from the present technique (Fig. 9a) reveals that the present technique provides more details of the flow and acoustic radiation fields. Also, due to short intervals between pulses, the present technique eliminates the formation of spurious fringes on the holographic image. Secondly, since the film plate is exposed twice with the flow on, the present technique filters out nonfluctuating density components within the flow. This, in turn, improves the sensitivity of the method. Thirdly, the previous technique has no time dependence in applying the two exposures, whereas the present method reveals optical data depending on the time separation between the two exposures.

V. Conclusions

The results obtained in the present investigation lead to the following conclusions.

A. $M=2.0$ Jet Flow

1) The observed characteristics of the radiated sound from fully expanded $M=2.0$ supersonic jets agrees with the previous observations that they may be mainly Mach wave radiation as modeled by "eddy-Mach wave" theory.

2) The optical records of fully expanded $M=2.0$ jet flow indicated that lower-frequency sound in supersonic jets is generated further downstream of the nozzle, 6-10 D, whereas the high-frequency components are generated principally close to nozzle exit, 2-4 D.

3) Under shock free as well as off-design operating conditions, the size and the apparent shape of the "closed-loop" fringe contours revealed information about turbulent fluctuations in the jet. As such, the results indicated that both eddy size and the magnitude of density fluctuations increased with increasing distance from the nozzle exit.

4) The observed features of supersonic nozzle flows operating at off-design modes seem to indicate that the dominant noise mechanism is an instability process related to the presence of shock cells in the flow.

B. $M=1.5$ Jet Flow

1) The observed characteristics within the acoustic and flow region of a fully expanded $M=1.5$ air jet suggested that the dominant waves radiated from shock free, low supersonic jets may not be the result of convected turbulent eddies but rather due to a hydrodynamic instability within the jet. Furthermore, this instability has the appearance of a coherent structure which is not confined to the mixing layer of the jet, but extends over the entire jet flow cross section.

2) The flowfield of the shock free $M=1.5$ jet exhibited a "large-scale spiraling structure" around the jet exhaust stream. The appearance of such a pattern at large pulse separations suggest that this kind of spiraling motion along the jet axis may be responsible for low-frequency sound radiation from supersonic jets.

3) The observation of "doughnut shaped closed-loop" fringe patterns under shock free as well as off-design conditions for the $M=1.5$ jet reveals that the scale and magnitude of density fluctuations increase with increasing distance from the nozzle exit.

4) For underexpanded $M=1.5$ jets, the passage of turbulent disturbances through the shock cells and also the interaction of the shock cells with the jet mixing layer seem to be the major noise source mechanism. For overexpanded jet flows under similar running conditions, however, there exists an instability within the flow region. The observed characteristic wavelength of this flow instability agrees with the discrete tone in the acoustic intensity spectrum of the jet.

5) The observed orderly fringe contour formation within the jet flow is indicative of the length scale of the flow instability. This length scale, which is in the order of the jet diameter, appears to increase with downstream distance.

For subsonic jets, the flow characteristics resemble those for low supersonic jets with the exception that the observed length scale of the orderly structure within the jet flow region is slightly larger, although still within the order of magnitude of the jet diameter.

References

[1] Lighthill, M. J., "On Sound Generated Aerodynamically. General Theory," *Proceedings of the Royal Society*, Vol. 211, 1952, p. 564.

[2] Lighthill, M. J., "On Sound Generated Aerodynamically. II Turbulence as a Source of Sound," *Proceedings of the Royal Society*, Vol. 222, 1954, p. 1.

[3] Phillips, O. M., "On the Generation of Sound by Supersonic Turbulent Shear Layers," *Journal of Fluid Mechanics*, Vol. 9, 1970.

[4] Schwartz, I. R., (Ed.), "Basic Aerodynamic Noise Research," NASA, SP-207, 1969.

[5] Sedelmikow, T., "The Frequency Spectrum of Noise of a Supersonic Jet," NASA TT F-538, 1979, p. 71.

[6] Tam, C.K.W., "Directional Acoustic Radiation from a Supersonic Jet Generated by Shear Layer Instability," *Journal of Fluid Mechanics*, Vol. 46, 1971, p. 757.

[7] Liu, J.T.C., "On Eddy Mach Wave Radiation Source Mechanism in the Jet Noise Problem," AIAA Paper 71-150, 1971.

[8] Lowson, M. V., "Shadowgraph Visualization of Noise from Cold Supersonic Jets," Wyle Lab Rept. No. WR-6, 1965.

[9] Eggers, J. M., "Velocity Profiles and Eddy Viscosity Distributions Downstream of a Mach 2.2 Nozzle Exhausting To Quiescent Air," NASA TN D-3601, 1966.

[10] Love, E. S., Grisby, C. E., et al., "Experimental and Theoretical Studies of Axisymmetric Free Jets," NASA TR-6, 1959.

[11] Salant, R. F., et al., "Holographic Study of the Mach Wave Field Generated by a Supersonic Turbulent Jet," *KIT Proceedings of the Purdue Noise Control Conference*, Lafayette, Ind., 1971.

[12] Ozkul, A., "Investigation of Acoustic Radiation From Supersonic Turbulent Jets by Double Pulse Holographic Interferometry," M.S. Thesis, The George Washington University, Hampton, Va., NASA, June 1971.

[13] Powell, A., "On the Mechanism of Choked Jet Noise," *Proceedings of the Physics Society*, Vol. 66-B, 1953, p. 1039.